INVESTIGATING EARLY DEVELOPMENT IN A MURINE MODEL OF DISSECTING ABDOMINAL AORTIC ANEURYSMS

Evan H. Phillips,[1] Ryan W. Grant,[2] and Craig J. Goergen[1]
*Weldon School of Biomedical Engineering,[1] Department of Nutrition Science,[2]
Purdue University, West Lafayette, Indiana, 47907, United States*

INTRODUCTION

Aortic rupture has an up to 90% chance of mortality due to hemorrhage in patients with aortic dissections or aneurysms. An aortic dissection is a tear in the wall of the aorta and an abdominal aortic aneurysm (AAA) is a localized pathological dilatation of the abdominal aorta. We have an incomplete understanding of these diseases because tissue is explanted only at a late stage. Therefore, there is an unmet need for treatment of early aortic disease.

Researchers have used several experimental animal models to investigate the pathology of aortic dissections and AAAs and to test potential therapeutics, as none currently exist. We use an established model of dissecting AAAs [1], the angiotensin II (AngII) apolipoprotein E knockout ($apoE^{-/-}$) model.

Our study <u>objective</u> was to investigate the early tissue- and molecular-level changes in this experimental model. We seek to determine whether pro-inflammatory factors and biomechanical changes are sufficient to cause pathological expansion in this model. The <u>long-term goal</u> of this work is to advance our understanding of the underlying factors that are associated with and potentially cause aortic dissection.

METHODS

We implanted male $apoE^{-/-}$ C57BL/6J mice at 12 weeks of age with AngII- and saline-loaded Alzet miniosmotic pumps with a dosing rate of 1000 ng/kg/min (DURECT Corp.). We screened the animals daily for the appearance of dissecting AAAs. On either the day of diagnosis or day 10 post-implantation, we acquired *in vivo* ultrasound data of aortic morphology (B-mode) and pulsatility (M-mode), using a 50 MHz centre frequency transducer (MS700) on the Vevo2100 system (FUJIFILM VisualSonics). We quantified effective maximum diameter, volume, and circumferential cyclic strain of each aorta. Effective maximum diameter (superior to the celiac artery) was determined using the equation for area of a circle and the measured aortic cross-sectional area. Volume was interpolated after axial 2D segmentation between the right renal artery and diaphragm. To calculate Green-Lagrange circumferential cyclic strain, we used the following equation where D_S are peak systolic and D_D end diastolic diameters [2-4]:

$$0.5 \times [(D_S/D_D)^2 - 1] \times 100\% \qquad (1)$$

We euthanized the mice with dissecting AAAs within 24 hours of diagnosis. The remaining mice, which did not show pathological expansion by day 10 (i.e. no dissecting AAA), were euthanized within 24 hours of this end point.

For gene expression analysis, total RNA of aortic segments (8 mm long) and periaortic fat was extracted using TRIzol reagent. cDNA was created to perform real-time polymerase chain reaction (RT-PCR) for two gene targets: interleukin-1β (IL-1β) and monocyte chemoattractant protein-1 (MCP-1) using SYBR Green reagent. A housekeeping gene (PPIA) was selected as an internal control in order to calculate relative delta C_T (cycle threshold) values.

An immunohistochemical procedure was carried out on frozen sections. We used primary mouse antibody for IL-1β, a biotinylated secondary antibody, an avidin-biotin complex kit for peroxidase staining, and metal-enhanced diaminobenzidine substrate.

All data are presented as mean ± standard error. A one-way ANOVA with a Tukey post hoc test was used for analysis of the ultrasound data. A Kruskal-Wallis test with Dunn's multiple comparisons test was used for non-parametric analysis of RT-PCR data. Significance was considered at $\alpha=0.05$.

RESULTS AND DISCUSSION

Ultrasound

We have previously shown that alongside an increase in volume, biomechanical and hemodynamic changes occur around the time of initial formation of dissecting AAAs [5].

In the present study, we have observed some morphological differences among three groups: (A) AngII-infused mice with dissecting AAAs, (B) AngII-infused mice without dissecting AAAs, and (C) saline-infused mice (Figure 1).
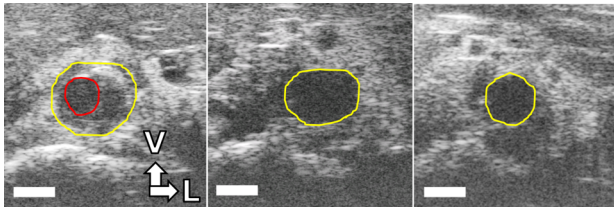

Figure 1: Short-axis images of the supraceliac aorta in mice with (left) and without (middle) a dissecting AAA after AngII infusion. The aorta of a saline-infused mouse is also shown (right). The outer vessel wall (yellow) and the true lumen (red) are outlined. V: ventral; L: left.
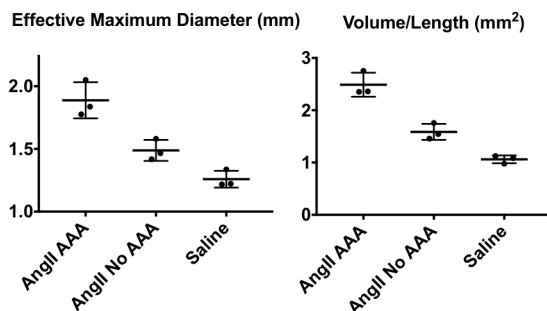

Figure 2: Effective maximum diameter (left) and volume/length values (right) across groups of mice with and without dissecting AAAs.

Effective maximum diameter at the study end points was significantly greater for mice in group A as compared to group B (25%) and more so as compared to group C (50%). Aortic volume/length values were also significantly different among all groups (Figure 2).

Aortic circumferential cyclic strain in group A was approximately 60% lower as compared to group B and 85% lower as compared to group C (Figure 3). Circumferential cyclic strain had an inverse trend with corresponding effective maximum diameter values (Pearson correlation coefficient, r = -0.762; p = 0.0171). Strain values for group A are similar to our previously published data [4, 5], confirming that the vessel walls of dissecting AAAs are stiffer (i.e. less pulsatile).
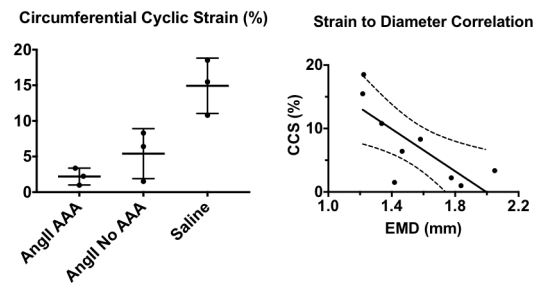

Figure 3: Green-Lagrange circumferential cyclic strain values (left) calculated based on equation 1. Inverse trend for circumferential cyclic strain (CCS) and effective maximum diameter (EMD) (right). 95% confidence bands (dashed lines) are displayed around a best-fit line (solid black line).

Histology and Immunohistochemistry

Our work seeks to evaluate the microstructural features (elastin breakage, separation of the medial and adventitial layers, and intramural thrombus [6, 7]) and pro-inflammatory factors [8, 9] present in AngII-infused mice. Previous studies have shown histological features at 28 days post-implantation [4, 7] and earlier [5, 6]. It is apparent that these features can develop quickly, underscoring the importance of the present study in which we have confined the collection of tissue within 24 hours of end points.

As shown by the example of an AngII-induced dissecting AAA in Figure 4, a large thrombus may form between the medial and adventitial layers of the aortic wall. As a result of a focal dissection (green arrow in Figure 5), the suprarenal aorta can substantially increase in size and expand leftward [7]. It follows therefore that the mice in group B are likely to have no point of complete focal dissection.
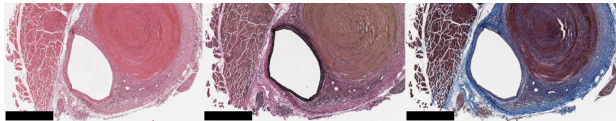

Figure 4: Example of an AngII-induced dissecting AAA in cross-section. Hematoxylin and eosin, Verhoeff Van-Gieson, and Masson's Trichrome stained sections are shown from left to right. Elastin is highlighted in black (middle) and collagen in blue (right). Scale bar: 500 µm.
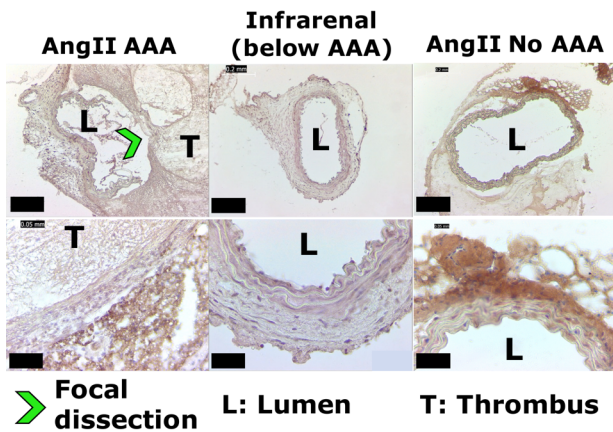

Figure 5: Examples of IL-1β staining in an AngII-induced dissecting AAA (left), in the infrarenal aorta of the same mouse (middle), and in the suprarenal aorta of an AngII-infused mouse without a dissecting AAA (right). Scale bars: 200 µm (top row) and 50 µm (bottom row).

The abundance of inflammatory markers in the aortic wall is of key consideration in the initial formation of AngII-induced dissecting AAAs. Our preliminary results suggest that the pro-inflammatory cytokine IL-1β is abundant within the adventitia of the suprarenal aortas of mice from groups A and B (Figure 5). This is in line with immunohistochemistry from a study by Usui et al. [9] that investigated the distribution of adventitial macrophages and IL-1β in $apoE^{-/-}$ mice after 7 days of AngII infusion.

Gene Expression Analysis

We conducted a baseline assessment of pro-inflammatory mRNA expression in non-AngII-infused mice. In $apoE^{-/-}$ mice as compared to wildtype mice, MCP-1 expression was increased 2.9 ± 1.0-fold (p=0.4025) and 5.4 ± 1.1-fold (p=0.0162) at the level of the suprarenal and infrarenal aorta, respectively (Figure 6). MCP-1 expression was increased 2.0 ± 0.9-fold and 2.2 ± 1.1-fold in suprarenal and infrarenal periaortic fat; however, these differences were not statistically significant, possibly due to small sample size. Low transcript levels of IL-1β were detected in $apoE^{-/-}$ and wildtype aortas and periaortic fat and we found no statistically significant difference among groups.
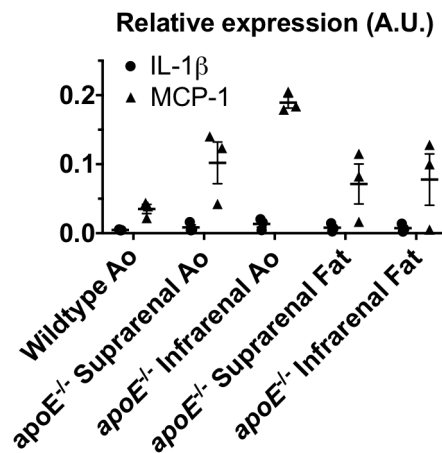

Figure 6: mRNA expression of IL-1β and MCP-1 in aortas and periaortic fat of non-AngII-infused $apoE^{-/-}$ mice. Levels in wildtype mouse aortas are also shown. A.U.: arbitrary units; Ao: aorta.

SUMMARY AND FUTURE DIRECTIONS

We have provided further evidence that morphological, biomechanical, and histological changes occur abruptly at the level of the suprarenal aorta in AngII-infused $apoE^{-/-}$ mice. Our ongoing work aims to extend these results

for a larger number of animals in order to identify how initial formation of dissecting AAAs occurs in this model. As well, gene expression and serum cytokine analysis will be performed to determine the significance of IL-1β and other associated factors in the disease process.

REFERENCES

[1]   A. Daugherty, M. W. Manning, and L. A. Cassis, "Angiotensin II promotes atherosclerotic lesions and aneurysms in apolipoprotein E-deficient mice.," *J. Clin. Invest.*, vol. 105, pp. 1605–1612, 2000.

[2]   J. D. Humphrey and S. L. Delange, *An Introduction to Biomechanics*. New York: Springer-Verlag, 2004.

[3]   C. J. Goergen, K. N. Barr, D. T. Huynh, J. R. Eastham-Anderson, G. Choi, M. Hedehus, et al., "In vivo quantification of murine aortic cyclic strain, motion, and curvature: implications for abdominal aortic aneurysm growth.," *J Magn Reson Imaging*, vol. 32, pp. 847–858, 2010.

[4]   E. H. Phillips, A. A. Yrineo, H. D. Schroeder, K. E. Wilson, J.-X. Cheng, and C. J. Goergen, "Morphological and Biomechanical Differences in the Elastase and AngII apoE-/- Rodent Models of Abdominal Aortic Aneurysms," *Biomed Res Int*, vol. 2015, p. 12, 2015.

[5]   E. Phillips, P. Di Achille, M. Bersi, J. Humphrey, and C. Goergen, "Multi-Modality Imaging Enables Detailed Hemodynamic Simulations in Dissecting Aneurysms in Mice.," *IEEE Trans Med Imaging*, ePub ahead of print, 2017.

[6]   K. Saraff, F. Babamusta, L. A. Cassis, and A. Daugherty, "Aortic dissection precedes formation of aneurysms and atherosclerosis in angiotensin II-infused, apolipoprotein E-deficient mice.," *Arterioscler. Thromb. Vasc. Biol.*, vol. 23, pp. 1621–1626, 2003.

[7]   C. J. Goergen, J. Azuma, K. N. Barr, L. Magdefessel, D. Y. Kallop, A. Gogineni, et al., "Influences of Aortic Motion and Curvature on Vessel Expansion in Murine Experimental Aneurysms," *Arterioscler. Thromb. Vasc. Biol.*, vol. 31, pp. 270–279, 2011.

[8]   R. Y. Cao, M. A. Adams, A. J. Habenicht, and C. D. Funk, "Angiotensin II-induced abdominal aortic aneurysm occurs independently of the 5-lipoxygenase pathway in apolipoprotein E-deficient mice.," *Prostaglandins Other Lipid Mediat.*, vol. 84, pp. 34–42, 2007.

[9]   F. Usui, K. Shirasuna, H. Kimura, K. Tatsumi, A. Kawashima, T. Karasawa, et al., "Inflammasome Activation by Mitochondrial Oxidative Stress in Macrophages Leads to the Development of Angiotensin II-Induced Aortic Aneurysm.," *Arterioscler. Thromb. Vasc. Biol.*, vol. 35, pp. 127–136, 2014.